

DIRECT REGULARIZED RECONSTRUCTION FOR THE THREE-DIMENSIONAL CALDERÓN PROBLEM

KIM KNUDSEN AND AKSEL KAASTRUP RASMUSSEN*

Technical University of Denmark
Department of Applied Mathematics and Computer Science
DK-2800 Kgs. Lyngby, Denmark

ABSTRACT. Electrical Impedance Tomography gives rise to the severely ill-posed Calderón problem of determining the electrical conductivity distribution in a bounded domain from knowledge of the associated Dirichlet-to-Neumann map for the governing equation. The uniqueness and stability questions for the three-dimensional problem were largely answered in the affirmative in the 1980's using complex geometrical optics solutions, and this led further to a direct reconstruction method relying on a non-physical scattering transform. In this paper, the reconstruction problem is taken one step further towards practical applications by considering data contaminated by noise. Indeed, a regularization strategy for the three-dimensional Calderón problem is presented based on a suitable and explicit truncation of the scattering transform. This gives a certified, stable and direct reconstruction method that is robust to small perturbations of the data. Numerical tests on simulated noisy data illustrate the feasibility and regularizing effect of the method, and suggest that the numerical implementation performs better than predicted by theory.

1. Introduction. Electrical Impedance Tomography (EIT) provides a noninvasive method of obtaining information on the electrical conductivity distribution of electric conductive media from exterior electrostatic measurements of currents and voltages. There are many applications in medical imaging including early detection of breast cancer [13, 58], hemorrhagic stroke detection [40, 24], pulmonary function monitoring [2, 22, 38] and targeting control in transcranial brain stimulation [52]. Applications also include industrial testing, for example, crack damage detection in cementitious structures [28, 25], and subsurface geophysical imaging [57]. The mathematical problem of EIT is called the Calderón problem and was first formulated by A.P. Calderón in 1980 [10] as follows: Consider a bounded Lipschitz domain $\Omega \subset \mathbb{R}^3$ filled with a conductor with a distribution $\gamma \in L^\infty(\Omega)$, $\gamma \geq c > 0$. Under the assumption of no sinks or sources of current in the domain, applying an electrical surface potential $f \in H^{1/2}(\partial\Omega)$ induces an electrical potential $u \in H^1(\Omega)$, which uniquely solves the conductivity equation

$$(1) \quad \begin{aligned} \nabla \cdot (\gamma \nabla u) &= 0 && \text{in } \Omega, \\ u &= f && \text{on } \partial\Omega. \end{aligned}$$

The Dirichlet-to-Neumann map $\Lambda_\gamma : H^{1/2}(\partial\Omega) \rightarrow H^{-1/2}(\partial\Omega)$ is defined as

$$\Lambda_\gamma f = \gamma \partial_\nu u|_{\partial\Omega},$$

2020 *Mathematics Subject Classification.* Primary: 35R30, 65J20; Secondary: 65N21.

Key words and phrases. Calderón problem, ill-posed problem, electrical impedance tomography, regularization, direct reconstruction algorithm.

* Corresponding author.

and associates a voltage potential on the boundary with a corresponding normal current flux. All pairs $(f, \gamma \partial_\nu u|_{\partial\Omega})$, or equivalently the Dirichlet-to-Neumann map, constitute the available data.

The forward problem is the problem of determining the Dirichlet-to-Neumann map given the conductivity, and it amounts to solving the boundary value problem (1) for all possible f . The Calderón problem now asks whether γ is uniquely determined by Λ_γ , and how to stably reconstruct γ from Λ_γ , if possible. Uniqueness and reconstruction were considered and solved for sufficiently regular conductivity distributions in dimension $n \geq 3$ in a series of papers [46, 44, 47, 56, 12]. The results are based on complex geometrical optics (CGO) solutions to a Schrödinger equation derived from (1). The first step of the reconstruction method is to recover the CGO solutions on $\partial\Omega$ by solving a weakly singular boundary integral equation with an exponentially growing kernel. The second step is obtaining the so-called non-physical scattering transform, which approximates in a large complex frequency limit the Fourier transform of $\gamma^{-1/2} \Delta \gamma^{1/2}$. Applying the inverse Fourier transform and solving a boundary value problem yields γ in the third step. Numerical algorithms following the scattering transform approach in dimension $n \geq 3$ have been developed by approximating the scattering transform [7, 36, 26, 8], by approximating the boundary integral equations [16], and for the full theoretical reconstruction algorithm [17]. A reconstruction algorithm for conductivity distributions close to a constant has been suggested, but not implemented [15].

A similar scattering transform approach combined with tools from complex analysis enables uniqueness and reconstruction [45] for the two-dimensional Calderón problem. More recently, a final affirmative answer was given to the question of uniqueness for a general bounded conductivity distribution in two dimensions [6]. Numerical algorithms and implementation for the two-dimensional problem have been considered [33, 34, 42, 43, 53, 54] and a regularization analysis and full implementation was given in [35]. We stress that in any practical case the Calderón problem is three-dimensional, since applying potentials on the boundary of a planar cross section of Ω leads to current flow leaving the plane.

The Calderón problem is known to be severely ill posed. Conditional stability estimates exist [3, 4] of the form

$$\|\gamma_1 - \gamma_2\|_{L^\infty(\Omega)} \leq f(\|\Lambda_{\gamma_1} - \Lambda_{\gamma_2}\|_Z),$$

for an appropriate function space Z and continuous function f with $f(0) = 0$ of logarithmic type. Furthermore, logarithmic stability is optimal [41]. While this is relevant for the theoretical reconstruction, there is no guarantee that a practically measured $\Lambda_\gamma^\varepsilon$ of a perturbed Dirichlet-to-Neumann map is the Dirichlet-to-Neumann map of any conductivity. We emphasize that in any practical case we can not have infinite-precision data, but rather a noisy finite approximation. Consequently, any computational algorithm for the problem needs regularization.

Classical regularization theory for inverse problems is given in [20, 32] with a focus on least squares formulations. A common approach to regularization for the Calderón problem is based on iterative regularized least-squares, and convergence of such methods is analyzed in [18, 49, 50, 37, 30] in the context of EIT. A quantitative comparison of CGO-based methods and iterative regularized methods is given in [26]. Reconstruction by statistical inversion is developed in [31, 19], where in the latter, the problem is posed in an infinite-dimensional Bayesian framework. A different statistical approach to the Calderón problem shows stable reconstruction

of the surface conductivity on a domain given noisy data [11]. Convergence estimates in probability of a statistical estimator (posterior mean) to the true conductivity given noisy data with a sufficiently small noise level are considered in [1].

In this paper we provide a direct CGO-based regularization strategy with an admissible parameter choice rule for reconstruction in the three-dimensional Calderón problem under the following assumptions:

Assumption 1. *For simplicity of exposition, we assume the domain of interest Ω is embedded in the unit ball in \mathbb{R}^3 . Furthermore, we assume $\partial\Omega$ is smooth.*

Assumption 2 (Parameter and data space). *We consider the forward map $F : D(F) \subset L^\infty(\Omega) \rightarrow Y$, $\gamma \mapsto \Lambda_\gamma$ with the following definition of $D(F)$. Let $\Pi > 0$ and $0 < \rho < 1$, then $\gamma \in D(F) \subset L^\infty(\Omega)$ satisfies*

$$\begin{aligned} \|\gamma\|_{C^2(\overline{\Omega})} &\leq \Pi, \\ \gamma(x) &\geq \Pi^{-1} \quad \text{for all } x \in \Omega, \\ \gamma(x) &\equiv 1 \quad \text{for } \text{dist}(x, \partial\Omega) < \rho, \end{aligned}$$

where we assume knowledge of Π and ρ . We continuously extend $\gamma \equiv 1$ outside Ω . The data space $Y \subset \mathcal{L}(H^{1/2}(\partial\Omega), H^{-1/2}(\partial\Omega))$ consists of bounded linear operators $\Lambda : H^{1/2}(\partial\Omega) \rightarrow H^{-1/2}(\partial\Omega)$ that are Dirichlet-to-Neumann alike in the sense

$$\Lambda(1) = 0,$$

$$\int_{\partial\Omega} (\Lambda f)(x) d\sigma(x) = 0 \quad \text{for every } f \in H^{1/2}(\partial\Omega).$$

We equip $D(F)$ and Y with the inherited norms $\|\cdot\|_{D(F)} = \|\cdot\|_{L^\infty(\Omega)}$ and $\|\cdot\|_Y = \|\cdot\|_{H^{1/2}(\partial\Omega) \rightarrow H^{-1/2}(\partial\Omega)}$.

There is no reason to believe that the regularity assumptions of γ is optimal, in fact, we expect that the strategy generalizes to the less regular setting of [12]. We recall the adaptation of the definitions in [20, 32] presented in [35] of a regularization strategy in the nonlinear setting. A family of continuous mappings $\mathcal{R}_\alpha : Y \rightarrow L^\infty(\Omega)$, parametrized by regularization parameter $0 < \alpha < \infty$, is called a regularization strategy for F if

$$(2) \quad \lim_{\alpha \rightarrow 0} \|\mathcal{R}_\alpha \Lambda_\gamma - \gamma\|_{L^\infty(\Omega)} = 0,$$

for each fixed $\gamma \in D(F)$. We define the perturbed Dirichlet-to-Neumann map as

$$\Lambda_\gamma^\varepsilon = \Lambda_\gamma + \mathcal{E},$$

with $\mathcal{E} \in Y$ and $\|\mathcal{E}\|_Y \leq \varepsilon$ for some $\varepsilon > 0$. We call ε the noise level, since we eventually simulate perturbations \mathcal{E} as random noise. Furthermore, a regularization strategy $\mathcal{R}_\alpha : Y \rightarrow L^\infty(\Omega)$, $0 < \alpha < \infty$, is called *admissible* if

$$(3) \quad \alpha(\varepsilon) \rightarrow 0 \quad \text{as } \varepsilon \rightarrow 0,$$

and for any fixed $\gamma \in \mathcal{D}(F)$ we have

$$(4) \quad \sup_{\Lambda_\gamma^\varepsilon \in Y} \{\|\mathcal{R}_{\alpha(\varepsilon)} \Lambda_\gamma^\varepsilon - \gamma\|_{L^\infty(\Omega)} \mid \|\Lambda_\gamma^\varepsilon - \Lambda_\gamma\|_Y \leq \varepsilon\} \rightarrow 0 \quad \text{as } \varepsilon \rightarrow 0.$$

The topology in which we require convergence is essential; we require convergence in strong operator topology, but not in norm topology. The main result of this paper is then as follows.

Theorem 1.1. *Suppose $\Pi > 0$ and $0 < \rho < 1$ are given and let $D(F)$ be as in Assumption 2. Then there exists $\varepsilon_0 > 0$, dependent only on Π and ρ such that the family \mathcal{R}_α defined by (30) is an admissible regularization strategy for F with the following choice of regularization parameter:*

$$(5) \quad \alpha(\varepsilon) = \begin{cases} (-1/11 \log(\varepsilon))^{-1/p} & \text{for } 0 < \varepsilon < \varepsilon_0, \\ \frac{\varepsilon}{\varepsilon_0} (-1/11 \log(\varepsilon_0))^{-1/p} & \text{for } \varepsilon \geq \varepsilon_0, \end{cases}$$

with $p > 3/2$.

This gives theoretical justification for practical reconstruction of the Calderón problem in three dimensions. This is the first deterministic regularization analysis for the three-dimensional Calderón problem known to the authors. Similar results have been shown for the related two-dimensional D-bar reconstruction [35], and we will in fact adopt the spectral truncation from there to our setting. This extension is non-trivial in part because there are no existence and uniqueness guarantees for the CGO solutions that are independent of the magnitude of the complex frequency in the three-dimensional case. In addition, while the two-dimensional D-bar method enjoys the continuous dependence of the solution to the D-bar equation on the scattering transform, it is not obvious when the frequency information of γ is stably recovered from the scattering transform corresponding to a perturbed Dirichlet-to-Neumann map in the three-dimensional case.

We denote the set of bounded linear operators between Banach spaces X and Y by $\mathcal{L}(X, Y)$ and use $\mathcal{L}(X) := \mathcal{L}(X, X)$. We denote the Euclidean matrix operator norm by $\|\cdot\|_N := \|\cdot\|_{\mathbb{C}^{(N+1)^2} \rightarrow \mathbb{C}^{(N+1)^2}}$. The operator norm of $A : H^s(\partial\Omega) \rightarrow H^t(\partial\Omega)$ is denoted by $\|A\|_{s,t}$. We reserve C for generic constants and C_1, C_2, \dots for constants of specific value. Finally, exponential functions of the form $e^{ix \cdot \zeta}$, $x \in \mathbb{R}^3$, $\zeta \in \mathbb{C}^3$, is denoted $e_\zeta(x)$.

In Section 2, the full non-linear reconstruction algorithm for the three-dimensional Calderón problem is given. Section 3 gives technical estimates regarding the boundary integral equation and the scattering transform and provides a regularizing method for perturbed data with ε sufficiently small. Then Section 4 extends continuously the method to a regularization strategy \mathcal{R}_α defined on Y and proves Theorem 1.1. In Section 5, the necessary numerical details concerning the representation of the Dirichlet-to-Neumann map and computation of the relevant norm are given. In addition, a noise model is given. Section 6 presents and discusses numerical results of noise tests with a piecewise constant conductivity distribution using an implementation given in [17], which is available from the corresponding author by request.

2. The full non-linear reconstruction method. Let $v = \gamma^{1/2}u$, then v is a solution to the Schrödinger equation

$$(6) \quad \begin{aligned} (-\Delta + q)v &= 0 & \text{in } \Omega, \\ v &= g & \text{on } \partial\Omega, \end{aligned}$$

with $q = \gamma^{-1/2}\Delta\gamma^{1/2}$ if and only if u is a solution to (1) with $f = \gamma^{-1/2}g$. Note in our setting $q = 0$ near $\partial\Omega$ and $q \equiv 0$ is extended continuously outside Ω and further $\Lambda_q g = \partial_\nu v = \Lambda_\gamma f$. The reconstruction method considered here is based on CGO solutions ψ_ζ to (6), which take the form

$$(7) \quad (-\Delta + q)\psi_\zeta = 0 \quad \text{in } \mathbb{R}^3,$$

satisfying $\psi_\zeta(x) = e^{ix \cdot \zeta}(1 + r_\zeta(x))$. Here the complex frequency $\zeta \in \mathbb{C}^3$ satisfies $\zeta \cdot \zeta = 0$ making $e^{ix \cdot \zeta}$ harmonic, and the remainder r_ζ belongs to certain weighted L^2 spaces. In the three-dimensional case, existence and uniqueness of CGO solutions have been shown for large complex frequencies,

$$(8) \quad |\zeta| > C_0 \|q\|_{L^\infty(\Omega)} =: D_q$$

for some constant $C_0 > 0$, or alternatively for $|\zeta|$ small [56, 15]. The analysis involves the Faddeev Green's function

$$G_\zeta(x) := e^{i\zeta \cdot x} g_\zeta(x) \quad g_\zeta(x) := \frac{1}{(2\pi)^3} \int_{\mathbb{R}^3} \frac{e^{ix \cdot \xi}}{|\xi|^2 + 2\xi \cdot \zeta} d\xi,$$

where g_ζ is defined in the sense of the inverse Fourier transform of a tempered distribution and interpretable as a fundamental solution of $(-\Delta - 2i\zeta \cdot \nabla)$. Boundedness of convolution by g_ζ on Ω is well known [56, 9, 51]:

$$(9) \quad \|g_\zeta * f\|_{L^2(\Omega)} \leq C |\zeta|^{s-1} \|f\|_{L^2(\Omega)}, \quad s \in \{0, 1, 2\},$$

where $|\zeta|$ is bounded away from zero, and C is independent of ζ and f .

The non-physical scattering transform is defined for all those ζ that give rise to a unique CGO solution ψ_ζ as

$$(10) \quad \mathbf{t}(\xi, \zeta) = \int_{\mathbb{R}^3} e^{-ix \cdot (\xi + \zeta)} \psi_\zeta(x) q(x) dx, \quad \xi \in \mathbb{R}^3.$$

It is useful to see the scattering transform as a non-linear Fourier transform of the potential q . Indeed, for $|\zeta| > D_q$ we have

$$(11) \quad |\mathbf{t}(\xi, \zeta) - \hat{q}(\xi)| \leq C \|q\|_{L^\infty(\Omega)}^2 |\zeta|^{-1},$$

for all $\xi \in \mathbb{R}^3$, where C is independent of ζ and q . Whenever $(\zeta + \xi) \cdot (\zeta + \xi) = 0$, integration by parts in (10) yields

$$(12) \quad \mathbf{t}(\xi, \zeta) = \int_{\partial\Omega} e^{-ix \cdot (\xi + \zeta)} (\Lambda_\gamma - \Lambda_1) \psi_\zeta(x) d\sigma(x),$$

where $d\sigma$ denotes the surface measure on $\partial\Omega$. For fixed $\xi \in \mathbb{R}^3$ this gives rise to the set $\mathcal{V}_\xi = \{\zeta \in \mathbb{C}^3 \setminus \{0\} \mid \zeta \cdot \zeta = 0, (\zeta + \xi) \cdot (\zeta + \xi) = 0\}$ parametrized by

$$(13) \quad \zeta(\xi) = \left(-\frac{\xi}{2} + \left(\kappa^2 - \frac{|\xi|^2}{4} \right)^{1/2} k^{\perp\perp} \right) + i\kappa k^\perp,$$

with $\kappa \geq \frac{|\xi|}{2}$ and $k^\perp, k^{\perp\perp} \in \mathbb{R}^3$ are unit vectors and $\{\xi, k^\perp, k^{\perp\perp}\}$ is an orthogonal set [17]. Note that for $\zeta(\xi) \in \mathcal{V}_\xi$ and $k \geq \frac{|\xi|}{2}$ we have $|\zeta(\xi)| = \sqrt{2}\kappa$; consequently $\lim_{\kappa \rightarrow \infty} |\zeta(\xi)| = \infty$.

For each fixed ζ the trace of the CGO solution $\psi_\zeta|_{\partial\Omega}$ is recoverable from the boundary integral equation

$$(14) \quad \psi_\zeta|_{\partial\Omega} + \mathcal{S}_\zeta (\Lambda_\gamma - \Lambda_1) (\psi_\zeta|_{\partial\Omega}) = e_\zeta|_{\partial\Omega},$$

where $\mathcal{S}_\zeta : H^{-1/2}(\partial\Omega) \rightarrow H^{1/2}(\partial\Omega)$ is the boundary single layer operator defined by

$$(\mathcal{S}_\zeta \varphi)(x) = \int_{\partial\Omega} G_\zeta(x - y) \varphi(y) d\sigma(y), \quad x \in \partial\Omega.$$

With \mathcal{S}_0 we denote the boundary single layer operator corresponding to the usual Green's function G_0 for the Laplacian. Occasionally we use the same notation when

$x \in \mathbb{R}^3 \setminus \partial\Omega$ and note it is well known that $\mathcal{S}_0\varphi$ and hence $\mathcal{S}_\zeta\varphi$ is continuous in \mathbb{R}^3 [14]. We let

$$B_\zeta := [I + \mathcal{S}_\zeta (\Lambda_\gamma - \Lambda_1)],$$

denote the boundary integral operator and we note the boundary integral equation (14) is a uniquely solvable Fredholm equation of the second kind for $|\zeta| > D_q$ [45]. This gives a method of recovering the Fourier transform of q in every frequency through the scattering transform (12) as $|\zeta| \rightarrow \infty$. This method of reconstruction for the Calderón problem in three dimensions was first explicitly given in [44, 47]. We summarize the method in three steps.

Method 1. CGO reconstruction in three dimensions

Step 1: Fix $\xi \in \mathbb{R}^3$ and solve the boundary integral equation (14) for all $\zeta(\xi) \in \mathcal{V}_\xi$.

Compute $\mathbf{t}(\xi, \zeta(\xi))$ by (12).

Step 2: Compute $\hat{q}(\xi)$ by

$$\lim_{|\zeta(\xi)| \rightarrow \infty} \mathbf{t}(\xi, \zeta(\xi)) = \hat{q}(\xi), \quad \xi \in \mathbb{R}^3,$$

and $q(x)$ by the inverse Fourier transform.

Step 3: Solve the boundary value problem

$$\begin{aligned} (-\Delta + q)\gamma^{1/2} &= 0 & \text{in } \Omega, \\ \gamma^{1/2} &= 1 & \text{on } \partial\Omega, \end{aligned}$$

and extract γ .

We remark that it is sufficient to solve the boundary integral equation in step 1 for a sequence $\{\zeta_k(\xi)\}_{k=1}^\infty$ of complex frequencies in \mathcal{V}_ξ that tends to infinity.

3. Regularized reconstruction by truncation. We continue by mimicking Method 1 with Λ_γ replaced by $\Lambda_\gamma^\varepsilon$ with ε small. We note that, in any case, using ψ_ζ with $|\zeta|$ large is impractical. Indeed, when using perturbed measurements naively in (12), the propagated perturbation of \mathbf{t} is ε multiplied with a factor exponentially growing in $|\zeta|$. This factor originates from the solution of the perturbed boundary integral equation

$$(15) \quad B_\zeta^\varepsilon(\psi_\zeta^\varepsilon|_{\partial\Omega}) := \psi_\zeta^\varepsilon|_{\partial\Omega} + \mathcal{S}_\zeta (\Lambda_\gamma^\varepsilon - \Lambda_1) (\psi_\zeta^\varepsilon|_{\partial\Omega}) = e_\zeta|_{\partial\Omega},$$

and in multiplication with $e^{-ix \cdot (\xi + \zeta(\xi))}$, see Lemma 3.3. We will show below that (15) is solvable for sufficiently small ε . To mitigate this exponential behavior we propose a reconstruction method that makes use of two coupled truncations: one of the complex frequency ζ and one of the real frequency of the signal q^ε , the perturbed analog of q . As we shall see, an upper bound of the magnitude $|\zeta(\xi)|$ determines an upper bound of the proximity of \mathbf{t} to \hat{q} , when using perturbed data. From (13) we have

$$|\zeta(\xi)| \geq \frac{|\xi|}{\sqrt{2}},$$

and hence fixing $|\zeta(\xi)|$ gives a bounded region in \mathbb{R}^3 , $|\xi| < M$ for some $M > 0$, in which \mathbf{t} can be computed. This gives the following method.

Method 2. Truncated CGO reconstruction in three dimensions

Step 1 $^\varepsilon$: Let $M = M(\varepsilon) > 0$ be determined by a sufficiently small ε . For each fixed ξ with $|\xi| < M$, take $\zeta(\xi) \in \mathcal{V}_\xi$ with an appropriate size determined by M and solve (15) to recover $\psi_\zeta^\varepsilon|_{\partial\Omega}$. Compute the truncated scattering transform by

$$\mathbf{t}_{M(\varepsilon)}^\varepsilon(\xi, \zeta(\xi)) := \begin{cases} \int_{\partial\Omega} e^{-ix \cdot (\xi + \zeta(\xi))} (\Lambda_\gamma^\varepsilon - \Lambda_1) \psi_\zeta^\varepsilon(x) d\sigma(x), & |\xi| < M(\varepsilon), \\ 0, & |\xi| \geq M(\varepsilon), \end{cases}$$

Step 2 $^\varepsilon$: Set $\widehat{q}^\varepsilon(\xi) := \mathbf{t}_{M(\varepsilon)}^\varepsilon(\xi, \zeta(\xi))$ and compute the inverse Fourier transform to obtain q^ε .

Step 3 $^\varepsilon$: Solve the boundary value problem

$$\begin{aligned} (-\Delta + q^\varepsilon)(\gamma^\varepsilon)^{1/2} &= 0 && \text{in } \Omega, \\ (\gamma^\varepsilon)^{1/2} &= 1 && \text{on } \partial\Omega. \end{aligned}$$

and extract γ^ε .

We call M the truncation radius and note it should depend on ε . Truncation of the scattering transform with truncation radius M is well known in regularization theory for the two-dimensional D-bar reconstruction method [35]. We can see the real truncation as a low-pass filtering in the frequency domain; this leads to additional smoothing in the spatial domain. Note that M determines the level of regularization and poses as a regularization parameter $\alpha = M^{-1}$ in the sense of (4).

In the following section we derive the required properties of \mathcal{S}_ζ , B_ζ^{-1} and $(B_\zeta^\varepsilon)^{-1}$. The invertibility of B_ζ^ε depends on the invertibility of the unperturbed boundary integral operator B_ζ , which is well known due to the mapping properties of \mathcal{S}_ζ . Although boundedness of \mathcal{S}_ζ and B_ζ^{-1} in the three-dimensional case follows by similar arguments to that of the two-dimensional [35], it is not immediately clear when $(B_\zeta^\varepsilon)^{-1}$ exists in the absence of existence and uniqueness guarantees of ψ_ζ for small $|\zeta|$. Neither is it clear under which circumstances q^ε approximates q as the noise level goes to zero. This is dealt with in Lemma 3.4 below by choosing a suitable rate, at which $|\zeta|$ and M goes to infinity as ε goes to zero.

3.1. The perturbed boundary integral equation. When $|\zeta|$ is bounded away from zero we can bound \mathcal{S}_ζ using the mapping properties (9) of convolution with g_ζ between Sobolev spaces defined on Ω . We note that one can give better bounds for arbitrarily small $|\zeta| < 1$ than the following result by considering the integral operator $\mathcal{S}_\zeta - \mathcal{S}_0$ with a smooth kernel, see [15, 35].

Lemma 3.1. *Let $\varphi \in H^{-1/2}(\partial\Omega)$ such that $\int_{\partial\Omega} \varphi(x) d\sigma(x) = 0$ and let $\zeta \in \mathbb{C}^3$ with $\zeta \cdot \zeta = 0$ and $|\zeta| > \beta > 0$. Then for the boundary single layer operator, \mathcal{S}_ζ , we have that*

$$\|\mathcal{S}_\zeta \varphi\|_{H^{1/2}(\partial\Omega)} \leq C_1 (1 + |\zeta|) e^{2|\zeta|} \|\varphi\|_{H^{-1/2}(\partial\Omega)},$$

where the constant C_1 is independent of ζ .

Proof. We follow [35]. Letting $x \in \mathbb{R}^3 \setminus \bar{\Omega}$ and introducing $u \in H^1(\Omega)$ with $\Delta u = 0$ and $\partial_\nu u = \varphi$ we write

$$\begin{aligned}
(\mathcal{S}_\zeta \varphi)(x) &= \int_{\partial\Omega} G_\zeta(x-y) \varphi(y) d\sigma(y), \\
&= \int_{\Omega} \nabla_y G_\zeta(x-y) \cdot \nabla u(y) dy, \\
&= -\nabla \cdot (G_\zeta * (\nabla u))(x), \\
&= -\nabla \cdot [e^{ix \cdot \zeta} (g_\zeta * (e^{-iy \cdot \zeta} \nabla u))](x),
\end{aligned}$$

using integration by parts, the chain rule and the fact that $G_\zeta(x - \cdot)$ is smooth in Ω . By the continuity of \mathcal{S}_ζ the above holds for $x \in \partial\Omega$ as well. Note from (9) and Leibniz' rule that

$$\|\nabla \cdot [e^{ix \cdot \zeta} (g_\zeta * (e^{-iy \cdot \zeta} \nabla u))]\|_{L^2(\Omega)} \leq C e^{2|\zeta|} \|\nabla u\|_{L^2(\Omega)},$$

and

$$\|\partial_{x_i} \nabla \cdot [e^{ix \cdot \zeta} (g_\zeta * (e^{-iy \cdot \zeta} \nabla u))]\|_{L^2(\Omega)} \leq C |\zeta| e^{2|\zeta|} \|\nabla u\|_{L^2(\Omega)},$$

for $i = 1, 2, 3$. This yields

$$\begin{aligned}
\|\mathcal{S}_\zeta \varphi\|_{H^{1/2}(\partial\Omega)} &\leq \|\nabla \cdot [e^{ix \cdot \zeta} (g_\zeta * (e^{-iy \cdot \zeta} \nabla u))]\|_{H^1(\Omega)}, \\
&\leq C(1 + |\zeta|) e^{2|\zeta|} \|\nabla u\|_{L^2(\Omega)}, \\
&\leq C(1 + |\zeta|) e^{2|\zeta|} \|\varphi\|_{H^{-1/2}(\partial\Omega)},
\end{aligned}$$

using the trace theorem and stability of the Neumann problem for u . Here C is dependent on β since $|\zeta| > \beta$. \square

We have the following estimate of B_ζ^{-1} . The main idea of the proof is to consider a solution $f \in H^{1/2}(\partial\Omega)$ to $B_\zeta f = h$ for some $h \in H^{1/2}(\partial\Omega)$ and then control the exponential component of f by creating a link to the CGO solutions of the Schrödinger equation.

Lemma 3.2. *For $\zeta \in \mathbb{C}^3 \setminus \{0\}$ with $\zeta \cdot \zeta = 0$ and $|\zeta| > D_q$ as in (8), the operator B_ζ is invertible with*

$$(16) \quad \|B_\zeta^{-1}\|_{1/2} \leq C_2(1 + |\zeta|) e^{2|\zeta|},$$

where C_2 is a constant depending only on the a priori knowledge Π and ρ .

Proof. We follow [35]. Using integration by parts note that $B_\zeta f = f + G_\zeta * (qv_f)$ on $\partial\Omega$, where $v_f \in H^1(\Omega)$ is the unique solution to

$$\begin{aligned}
(-\Delta + q)v_f &= 0 && \text{in } \Omega, \\
v_f &= f && \text{on } \partial\Omega.
\end{aligned}$$

To bound f we bound v_f by writing $v_f = v - u^{\text{exp}}$ with

$$\begin{aligned}
\Delta v &= 0 && \text{in } \Omega, \\
v &= B_\zeta f && \text{on } \partial\Omega,
\end{aligned}$$

and $u^{\text{exp}} := G_\zeta * (qv_f)$. From the stability property of the Dirichlet problem it is sufficient to bound u^{exp} in terms of v . Note $(-\Delta + q)u^{\text{exp}} = qv$ and hence conjugating with exponentials yields the equation in \mathbb{R}^3 ,

$$(17) \quad (-\Delta - 2i\zeta \cdot \nabla + q)u = qve^{-ix \cdot \zeta},$$

where we set $u = e^{-ix \cdot \zeta} u^{\text{exp}}$. It is well known that u is the unique solution among functions in certain weighted $L^2(\mathbb{R}^3)$ -spaces satisfying

$$\|u\|_{L^2(\Omega)} \leq C \|q\|_{L^\infty} \frac{e^{|\zeta|}}{|\zeta|} \|v\|_{L^2(\Omega)},$$

whenever $|\zeta| > D_q$, see [56]. Indeed, convolution with g_ζ on both sides of (17) gives

$$u = g_\zeta * (-qu + qve^{-ix \cdot \zeta}),$$

which upgrades the estimate to

$$\|u\|_{H^1(\Omega)} \leq C \|q\|_{L^\infty} e^{|\zeta|} \|v\|_{L^2(\Omega)},$$

using (9). Now the estimate (16) follows straightforwardly from the trace theorem. \square

We note that a main difference between the boundary integral equation in two dimensions and three dimensions is the possible existence of a certain ζ for which there exists no unique CGO solutions to (7). The next result shows that Lemma 3.1 and Lemma 3.2 implies solvability of the perturbed boundary integral equation using a Neumann series argument on the form

$$B_\zeta^\varepsilon = I + \mathcal{S}_\zeta(\Lambda_\gamma^\varepsilon - \Lambda_\gamma) + \mathcal{S}_\zeta(\Lambda_\gamma - \Lambda_1) = [I + A_\zeta^\varepsilon]B_\zeta,$$

where $A_\zeta^\varepsilon := \mathcal{S}_\zeta \mathcal{E} B_\zeta^{-1}$ is a bounded operator in $H^{1/2}(\partial\Omega)$. It is clear from Lemma 3.2 that q fixes a lower bound for $|\zeta|$, for which B_ζ is certain to be invertible. When the noise level is sufficiently small such that $D_q < |\zeta| < R(\varepsilon)$, for some R , we may invert B_ζ^ε . We have the following result.

Lemma 3.3. *Let $R = R(\varepsilon) := -\frac{1}{6} \log \varepsilon$, and suppose $D_q < |\zeta| < R(\varepsilon_1)$ for some $0 < \varepsilon_1 < 1$. Then there exists $0 < \varepsilon_2 \leq \varepsilon_1$ for which B_ζ^ε is invertible whenever $0 < \varepsilon < \varepsilon_2$. Furthermore we have the estimate*

$$\|\psi_\zeta^\varepsilon - \psi_\zeta\|_{H^{1/2}(\partial\Omega)} \leq C_3 \varepsilon (1 + R)^4 e^{7R},$$

where C_3 is a constant depending only on the a priori knowledge of Π and ρ .

Proof. Since $\mathcal{E} \in Y$, it maps onto trace functions that have zero mean on the boundary. Then from Lemma 3.1 and Lemma 3.2 we find

$$\begin{aligned} \|A_\zeta^\varepsilon\|_{1/2} &= \|\mathcal{S}_\zeta \mathcal{E} B_\zeta^{-1}\|_{1/2} \leq C_1 C_2 \varepsilon (1 + R)^2 e^{4R}, \\ (18) \qquad \qquad \qquad &\leq C \varepsilon e^{5R}, \end{aligned}$$

where we have absorbed the polynomial in R into the exponential and thereby obtained a new constant. By the definition of R , we note the right-hand side of (18) goes to zero as ε goes to zero, and hence there exists a $0 < \varepsilon_2 \leq \varepsilon_1$ such that $\|A_\zeta^\varepsilon\|_{1/2} < \frac{1}{2}$. Then by a Neumann series argument, $I + A_\zeta^\varepsilon$ is invertible with $\|(I + A_\zeta^\varepsilon)^{-1}\|_{1/2} < 2$, and $(B_\zeta^\varepsilon)^{-1} = B_\zeta^{-1} [I + A_\zeta^\varepsilon]^{-1}$. From the boundary integral equations we have $\psi_\zeta = B_\zeta^{-1}(e_\zeta|_{\partial\Omega})$ and $\psi_\zeta^\varepsilon = (B_\zeta^\varepsilon)^{-1}(e_\zeta|_{\partial\Omega})$. Then with the use of Lemma 3.2 we have for $0 < \varepsilon < \varepsilon_2$

$$\begin{aligned} \|\psi_\zeta^\varepsilon\|_{H^{1/2}(\partial\Omega)} &\leq \|(B_\zeta^\varepsilon)^{-1}(e_\zeta|_{\partial\Omega})\|_{H^{1/2}(\partial\Omega)}, \\ (19) \qquad \qquad \qquad &\leq 2 \|B_\zeta^{-1}\|_{1/2} \|e^{ix \cdot \zeta}\|_{H^{1/2}(\partial\Omega)}, \end{aligned}$$

$$(20) \qquad \qquad \qquad \leq C(1 + |\zeta|)^2 e^{3|\zeta|}.$$

With the use of Lemma 3.2 we have for $0 < \varepsilon < \varepsilon_2$

$$\begin{aligned} \|(B_\zeta^\varepsilon)^{-1} - B_\zeta^{-1}\|_{1/2} &= \|B_\zeta^{-1}[(I + A_\zeta^\varepsilon)^{-1} - I]\|_{1/2}, \\ &\leq \|B_\zeta^{-1}\|_{1/2} \|(I + A_\zeta^\varepsilon)^{-1} [I - (I + A_\zeta^\varepsilon)]\|_{1/2}, \\ &\leq \|B_\zeta^{-1}\|_{1/2} \|(I + A_\zeta^\varepsilon)^{-1}\|_{1/2} \|A_\zeta^\varepsilon\|_{1/2}, \\ &\leq 2C_1 C_2^2 \varepsilon (1 + R)^3 e^{6R}. \end{aligned}$$

Finally we obtain

$$\begin{aligned} \|\psi_\zeta^\varepsilon - \psi_\zeta\|_{H^{1/2}(\partial\Omega)} &= \|[(B_\zeta^\varepsilon)^{-1} - B_\zeta^{-1}]e_\zeta\|_{H^{1/2}(\partial\Omega)}, \\ &\leq \|(B_\zeta^\varepsilon)^{-1} - B_\zeta^{-1}\|_{1/2} \|e^{ix \cdot \zeta}\|_{H^{1/2}(\partial\Omega)}, \\ (21) \quad &\leq 2C_1 C_2^2 \varepsilon (1 + R)^4 e^{7R}, \end{aligned}$$

for $0 < \varepsilon < \varepsilon_2$. □

3.2. Truncation of the scattering transform. We now show that fixing the magnitude of the complex frequency $|\zeta(\xi)| = (M(\varepsilon))^p$ with $p > 3/2$, enables control over the proximity of the truncated scattering transform $\mathbf{t}_M^\varepsilon(\cdot, \zeta)$ to \hat{q} for small noise levels. This choice is justified from the following result.

Lemma 3.4. *Let $M(\varepsilon) = (-1/11 \log(\varepsilon))^{1/p}$ be a truncation radius depending on ε and some exponent $p > 3/2$. Fix $\xi \in \mathbb{R}^3$ with $|\xi| < M(\varepsilon)$, suppose $\zeta(\xi) \in \mathcal{V}_\xi$ with*

$$|\zeta(\xi)| = (M(\varepsilon))^p = -\frac{1}{11} \log(\varepsilon)$$

and let ε_2 be defined as in the proof of Lemma 3.3. Further fix $q \in L^\infty(\Omega)$ corresponding to a $\gamma \in D(F)$. Then \mathbf{t}_M^ε is well defined by (29) for $0 < \varepsilon < \varepsilon_2$ and

$$\lim_{\varepsilon \rightarrow 0} \|\mathbf{t}_{M(\varepsilon)}^\varepsilon - \hat{q}\|_{L^2(\mathbb{R}^3)} = 0.$$

Proof. For (i) fix first $|\xi| < M(\varepsilon)$ and note first by the triangle inequality that

$$(22) \quad |\mathbf{t}_{M(\varepsilon)}^\varepsilon(\xi, \zeta(\xi)) - \hat{q}(\xi)| \leq |\mathbf{t}_{M(\varepsilon)}^\varepsilon(\xi, \zeta(\xi)) - \mathbf{t}(\xi, \zeta(\xi))| + |\mathbf{t}(\xi, \zeta(\xi)) - \hat{q}(\xi)|.$$

By Lemma 3.3 there exists a unique solution ψ_ζ^ε to the perturbed boundary integral equation and hence \mathbf{t}_M^ε is well defined. Using (20) and (21), we find the following, in which we set $R = R(\varepsilon)$, $M = M(\varepsilon)$ and $\zeta = \zeta(\xi)$ for simplicity of exposition,

$$\begin{aligned} |\mathbf{t}_M^\varepsilon(\xi, \zeta) - \mathbf{t}(\xi, \zeta)| &= \left| \int_{\partial\Omega} e^{-ix \cdot (\xi + \zeta)} [(\Lambda_\gamma^\varepsilon - \Lambda_1) \psi_\zeta^\varepsilon(x) - (\Lambda_\gamma - \Lambda_1) \psi_\zeta(x)] d\sigma(x) \right|, \\ (23) \quad &\leq \|e^{-ix \cdot (\xi + \zeta)}\|_{H^{1/2}(\partial\Omega)} \|\Lambda_\gamma - \Lambda_1\|_Y \|\psi_\zeta^\varepsilon - \psi_\zeta\|_{H^{1/2}(\partial\Omega)} \\ &\quad + \|e^{-ix \cdot (\xi + \zeta)}\|_{H^{1/2}(\partial\Omega)} \|\Lambda_\gamma^\varepsilon - \Lambda_\gamma\|_Y \|\psi_\zeta^\varepsilon\|_{H^{1/2}(\partial\Omega)}, \\ &\leq C(1 + |\zeta|) e^{|\zeta|} \left[\varepsilon(1 + |\zeta|)^4 e^{7|\zeta|} + \varepsilon(1 + |\zeta|)^2 e^{3|\zeta|} \right], \end{aligned}$$

where we use the fact that $\|\Lambda_\gamma - \Lambda_1\|_Y \leq C$, where C depends only on Π by the continuity of the forward map $\gamma \mapsto \Lambda_\gamma$. Then,

$$|\mathbf{t}_M^\varepsilon(\xi, \zeta) - \mathbf{t}(\xi, \zeta)| \leq C\varepsilon e^{9|\zeta|}.$$

Using (22) and the property (11) we conclude for $|\xi| < M(\varepsilon)$ that

$$(24) \quad |\mathbf{t}_M^\varepsilon(\xi, \zeta) - \hat{q}(\xi)| \leq C\varepsilon e^{9|\zeta|} + C|\zeta|^{-1}.$$

Then for (ii), using the triangle inequality and (24) we find

$$\begin{aligned}
\|\mathbf{t}_M^\varepsilon - \hat{q}\|_{L^2(\mathbb{R}^3)} &\leq \|\mathbf{t}_M^\varepsilon - \hat{q}\|_{L^2(|\xi| < M)} + \|\hat{q}\|_{L^2(|\xi| \geq M)}, \\
&\leq C(\varepsilon e^{9|\zeta|} + M^{-p}) \left(\int_0^M r^2 dr \right)^{1/2} + \|\hat{q}\|_{L^2(|\xi| \geq M)}, \\
&\leq C(\varepsilon e^{10|\zeta|} + M^{3/2-p}) + \|\hat{q}\|_{L^2(|\xi| \geq M)}, \\
&\leq C\varepsilon^{1/11} + C(-1/11 \log(\varepsilon))^{3/2-p} + \|\hat{q}\|_{L^2(|\xi| \geq M)},
\end{aligned}$$

for $0 < \varepsilon < \varepsilon_2$. Since $q \in L^\infty(\Omega)$ is compactly supported in Ω , we have $q \in L^2(\mathbb{R}^3)$, and hence the energy of the tail of \hat{q} converges to zero as $M(\varepsilon)$ goes to infinity. The result follows as $p > 3/2$. \square

One may obtain an explicit decay of \hat{q} by assuming a certain regularity of q . Notice the proof above works fine with the choice $|\zeta| = K_1 M^p + K_2$ for some $0 < K_1 < 1$, $K_2 > 0$ and $p > 3/2$. A user may choose among such $|\zeta|$ freely, with $p = 3/2$ being the critical choice. We now prove that γ^ε exists and is unique and that the propagated reconstruction error tends to zero if $\varepsilon \rightarrow 0$, given $\|q^\varepsilon - q\|_{L^2(\Omega)}$ is sufficiently small. This is possible in $H^2(\Omega)$ by a Neumann series argument and elliptic regularity. For the boundary value problem

$$\begin{aligned}
(-\Delta + q^\varepsilon)u &= f && \text{in } \Omega, \\
u &= 0 && \text{on } \partial\Omega,
\end{aligned}$$

with $f \in L^2(\Omega)$, we introduce the notation $L^\varepsilon : H_0^1(\Omega) \cap H^2(\Omega) \rightarrow L^2(\Omega)$, $L^\varepsilon : u \mapsto f$, defined for any $q^\varepsilon \in L^2(\Omega)$ and then note

$$\gamma^\varepsilon = [(L^\varepsilon)^{-1}(-q^\varepsilon) + 1]^2,$$

whenever $(L^\varepsilon)^{-1}$ exists.

Lemma 3.5. *Let $q = \Delta\gamma^{1/2}\gamma^{-1/2}$ be a potential with $\gamma \in D(F)$. Then there exists a $0 < \varepsilon_3 < 1$ such that for $0 < \varepsilon < \min(\varepsilon_2, \varepsilon_3) =: \varepsilon_0$ the boundary value problem*

$$\begin{aligned}
(-\Delta + q^\varepsilon)(\gamma^\varepsilon)^{1/2} &= 0 && \text{in } \Omega, \\
(\gamma^\varepsilon)^{1/2} &= 1 && \text{on } \partial\Omega,
\end{aligned} \tag{25}$$

has a unique solution in $H^2(\Omega)$. Furthermore the following inequality holds

$$\|\gamma^{1/2} - (\gamma^\varepsilon)^{1/2}\|_{H^2(\Omega)} \leq C_4 \|q - q^\varepsilon\|_{L^2(\Omega)}, \tag{26}$$

where C_4 is dependent only on Π and ρ .

Proof. Note $(-\Delta + q)^{-1}$ exists and is bounded for $L^2(\Omega)$ into $H_0^1(\Omega) \cap H^2(\Omega)$ with

$$\|u\|_{H^2(\Omega)} \leq C \|f\|_{L^2(\Omega)}, \tag{27}$$

by elliptic regularity [21]. Here C is dependent only on Π . We construct

$$L^\varepsilon u = (-\Delta + q)[I + (-\Delta + q)^{-1}(q^\varepsilon - q)]u,$$

and seek boundedness of $(-\Delta + q)^{-1}(q^\varepsilon - q)$ in $H^2(\Omega)$ as our goal. For any $u \in H^2(\Omega)$

$$\|(-\Delta + q)^{-1}(q^\varepsilon - q)u\|_{H^2(\Omega)} \leq C \|q^\varepsilon - q\|_{L^2(\Omega)} \|u\|_{H^2(\Omega)},$$

using (27) and Sobolev embedding theory. By Lemma 3.4, there exists a $0 < \varepsilon_3 < 1$ such that for all $0 < \varepsilon < \min(\varepsilon_2, \varepsilon_3)$

$$\|(-\Delta + q)^{-1}(q^\varepsilon - q)\|_{H^2(\Omega) \rightarrow H^2(\Omega)} \leq C \|q^\varepsilon - q\|_{L^2(\Omega)} < \frac{1}{2}.$$

Hence $(L^\varepsilon)^{-1}$ exists and is uniformly bounded with respect to $0 < \varepsilon \leq \varepsilon_0$. Finally, since $\gamma \in L^\infty(\Omega)$ we have $(q^\varepsilon - q)\gamma^{1/2} \in L^2(\Omega)$, and by solving

$$\begin{aligned} L^\varepsilon(\gamma^{1/2} - (\gamma^\varepsilon)^{1/2}) &= (q^\varepsilon - q)\gamma^{1/2} && \text{in } \Omega \\ \gamma^{1/2} - (\gamma^\varepsilon)^{1/2} &= 0 && \text{on } \partial\Omega, \end{aligned}$$

we obtain the estimate (26). \square

We conclude that γ^ε of Method 2 exists uniquely and approximates γ in the $H^2(\Omega)$ -norm, whenever $\varepsilon < \varepsilon_0$.

4. Extending the method to a regularization strategy. From the definition of an admissible regularization strategy it is clear \mathcal{R}_α must be defined on Y and not only an ε_0 -neighborhood of $F(\mathcal{D}(F))$. However, $(B_\xi^\varepsilon)^{-1}$ and $(L^\varepsilon)^{-1}$ exists only for small enough ε . We confront this by extending these operators to $(B_\xi^\varepsilon)^\dagger_\alpha$ and $(L^\varepsilon)^\dagger_\alpha$ coinciding with $(B_\xi^\varepsilon)^{-1}$ and $(L^\varepsilon)^{-1}$ for $\varepsilon < \varepsilon_0$, such that \mathcal{R}_α is continuous and well defined on Y . There are several ways to obtain such extensions, however we will follow [35] and construct explicit pseudoinverses by means of functional calculus. Define the normal operator

$$S_\xi^\varepsilon := (B_\xi^\varepsilon)^*(B_\xi^\varepsilon) \in \mathcal{L}(H^{1/2}(\partial\Omega)),$$

where $(B_\xi^\varepsilon)^*$ is the adjoint operator of $(B_\xi^\varepsilon) \in \mathcal{L}(H^{1/2}(\partial\Omega))$. Similarly we define

$$T_\xi^\varepsilon := (L^\varepsilon)^*(L^\varepsilon) \in \mathcal{L}(L^2(\Omega)).$$

Let h_α^1 and h_α^2 be two real functions defined for $0 < \alpha < \infty$ as

$$h_\alpha^i(t) := \begin{cases} t^{-1} & \text{for } t > \kappa_i(\alpha), \\ \kappa_i(\alpha)^{-1} & \text{for } t \leq \kappa_i(\alpha), \end{cases}$$

for $i = 1, 2$ with $\kappa_i(\alpha) = \frac{1}{4}r_i(\alpha)^2$, where we will see below the estimates (26) and (31) motivates the definition

$$r_i(\alpha) := \begin{cases} \frac{1}{C_2(1+\alpha^{-p})e^{2\alpha^{-p}}} & \text{for } i = 1, \\ \frac{1}{C_4} & \text{for } i = 2, \end{cases}$$

with $p > 3/2$. We define the α -pseudoinverses $(B_\xi^\varepsilon)^\dagger_\alpha$ of B_ξ^ε and $(L^\varepsilon)^\dagger_\alpha$ of L^ε for any $0 < \alpha < \infty$ as

$$\begin{aligned} (B_\xi^\varepsilon)^\dagger_\alpha &:= h_\alpha^1(S_\xi^\varepsilon)(B_\xi^\varepsilon)^*, \\ (L^\varepsilon)^\dagger_\alpha &:= h_\alpha^2(T_\xi^\varepsilon)(L^\varepsilon)^*, \end{aligned}$$

where the operators $h_\alpha^1(S_\xi^\varepsilon)$ in $\mathcal{L}(H^{1/2}(\partial\Omega))$ and $h_\alpha^2(T_\xi^\varepsilon)$ in $\mathcal{L}(L^2(\Omega))$ are defined in the sense of continuous functional calculus (see for example [48, 55]) and depend continuously on S_ξ^ε and T_ξ^ε , respectively (see for example [35, Lemma 3.1]). This implies $\Lambda_\gamma^\varepsilon \mapsto (B_\xi^\varepsilon)^\dagger_\alpha$ and $q^\varepsilon \mapsto (L^\varepsilon)^\dagger_\alpha$ are continuous mappings. Explicitly, for a self-adjoint operator $S : \mathcal{H} \rightarrow \mathcal{H}$ for a Hilbert space \mathcal{H} we set

$$(28) \quad h_\alpha^i(S) = \int_{\sigma(S)} h_\alpha^i(\lambda) dP(\lambda),$$

where $\sigma(S) \subset \mathbb{C}$ denotes the spectrum of S , and P is a spectral measure on $\sigma(S)$.

Method 3. Regularized CGO reconstruction in three dimensions

Step 1_α: Given $\alpha > 0$, set $M = \alpha^{-1}$. For each $|\xi| < M$ take $\zeta(\xi) \in \mathcal{V}_\xi$ with $|\zeta(\xi)| = M^p$ for $p > 3/2$ and define

$$\tilde{\psi}_\alpha := (B_\zeta^\varepsilon)^\dagger_\alpha(e_\zeta|_{\partial\Omega})$$

and compute the truncated scattering transform $\mathbf{t}_\alpha(\xi, \zeta(\xi))$ for $\zeta(\xi)$ in \mathcal{V}_ξ by

$$(29) \quad \tilde{\mathbf{t}}_\alpha(\xi, \zeta(\xi)) = \begin{cases} \int_{\partial\Omega} e^{-ix \cdot (\xi + \zeta(\xi))} (\Lambda_\gamma^\varepsilon - \Lambda_1) \tilde{\psi}_\alpha(x) d\sigma(x) & |\xi| < M, \\ 0 & |\xi| \geq M \end{cases}$$

Step 2_α: Define $\widehat{q_\alpha}(\xi) := \tilde{\mathbf{t}}_\alpha(\xi, \zeta(\xi))$ and compute the inverse Fourier transform to obtain q_α .

Step 3_α: Solve the boundary value problem (25) by computing $(L^\varepsilon)^\dagger_\alpha(-q_\alpha)$ and set

$$(30) \quad \mathcal{R}_\alpha \Lambda_\gamma^\varepsilon := [(L^\varepsilon)^\dagger_\alpha(-q_\alpha) + 1]^2$$

Proof of Theorem 1.1. Given $\Lambda_\gamma^\varepsilon$ in Y we have

$$\begin{aligned} |\tilde{\mathbf{t}}_\alpha(\xi, \zeta(\xi))| &\leq \left| \int_{\partial\Omega} e^{-ix \cdot (\xi + \zeta)} [(\Lambda_\gamma^\varepsilon - \Lambda_\gamma) \tilde{\psi}_\alpha(x) + (\Lambda_\gamma - \Lambda_1) \tilde{\psi}_\alpha(x)] d\sigma(x) \right|, \\ &\leq \|e^{-ix \cdot (\xi + \zeta)}\|_{H^{1/2}(\partial\Omega)} \|\Lambda_\gamma^\varepsilon - \Lambda_\gamma\|_Y \|\tilde{\psi}_\alpha\|_{H^{1/2}(\partial\Omega)} \\ &\quad \|e^{-ix \cdot (\xi + \zeta)}\|_{H^{1/2}(\partial\Omega)} \|\Lambda_\gamma - \Lambda_1\|_Y \|\tilde{\psi}_\alpha\|_{H^{1/2}(\partial\Omega)}, \\ &< \infty, \end{aligned}$$

for all $\xi \in \mathbb{R}^3$, since $(B_\zeta^\varepsilon)^\dagger_\alpha$ is bounded in $H^{1/2}(\partial\Omega)$. Then by compact support $\tilde{\mathbf{t}}_\alpha \in L^2(\mathbb{R}^3)$. It follows the inverse Fourier transform of this object is well defined and hence the family of operators \mathcal{R}_α is well defined. Using the continuity of the maps $\Lambda_\gamma^\varepsilon \mapsto (B_\zeta^\varepsilon)^\dagger_\alpha$ and $q_\alpha \mapsto (L^\varepsilon)^\dagger_\alpha$, a parallel estimation to (23) and the linearity and boundedness of the inverse Fourier transform in $L^2(\mathbb{R}^3)$, it is clear that \mathcal{R}_α is a family of continuous mappings. Now recall from Lemma 3.2 and (19) that for $0 < \varepsilon < \varepsilon_0$ we have that

$$(31) \quad \|(B_\zeta^\varepsilon)\|_{1/2}^{-1} \leq \|(B_\zeta^\varepsilon)^{-1}\|_{1/2} \leq 2C_2(1 + |\zeta|)e^{2|\zeta|}.$$

Set $|\zeta| = \alpha^{-p}$ and note

$$S_\zeta^\varepsilon \geq \frac{1}{4} r_1(\alpha)^2 I.$$

By definition of the α -pseudoinverse and (28) we have that $(B_\zeta^\varepsilon)^\dagger_\alpha = (B_\zeta^\varepsilon)^{-1}$ for $0 < \varepsilon < \varepsilon_0$, and hence $\tilde{\psi}_\alpha = \psi_\zeta^\varepsilon$ is unique. It follows by Lemma 3.4 that $\tilde{\mathbf{t}}(\cdot, \zeta(\cdot))$ is well defined and $q_\alpha = q^\varepsilon$ converges to q as ε goes to zero. Conversely, for $0 < \varepsilon < \varepsilon_0$ we have $(L^\varepsilon)^\dagger_\alpha = (L^\varepsilon)^{-1}$, and hence by Lemma 3.5 and the Sobolev embedding $H^2(\Omega) \subset C^0(\overline{\Omega})$, (4) is satisfied. Note also the weaker requirement (2) follows analogously. The property (3) is satisfied by (5). \square

A direct consequence of the truncation of the scattering transform is the following property of the reconstruction $\mathcal{R}_\alpha(\varepsilon) \Lambda_\gamma^\varepsilon$ for sufficiently small ε . The regularized reconstructions are as regular as Ω .

Proposition 1. *Suppose $\Lambda_\gamma^\varepsilon = \Lambda_\gamma + \mathcal{E}$ with $\|\mathcal{E}\|_Y \leq \varepsilon < \varepsilon_0$. Then $\mathcal{R}_\alpha(\varepsilon) \Lambda_\gamma^\varepsilon \in C^\infty(\overline{\Omega})$.*

Proof. Since $\tilde{\mathbf{t}}_\alpha(\cdot, \zeta(\cdot)) \in L^1(\mathbb{R}^3)$ has compact support, it follows q_α is smooth. Since $\partial\Omega$ is smooth, it follows $\mathcal{R}_\alpha \Lambda_\gamma^\varepsilon \in C^\infty(\overline{\Omega})$ by elliptic regularity [21]. \square

5. Computational methods. In this section we outline methods of representing and computing the Dirichlet-to-Neumann map numerically and consider the discretization of the boundary integral equations. We assume $\Omega = B(0, 1)$ in order to utilize spherical harmonics in representation of functions on $\partial\Omega$.

5.1. Representation and computation of the Dirichlet-to-Neumann map.

We consider the Hilbert space $H^s(\partial\Omega)$, $s > 0$, defined as the space of all functions f in $L^2(\partial\Omega)$ that satisfy

$$(32) \quad \|f\|_{L^2(\partial\Omega)}^2 + \|(-\Delta_S)^{s/2} f\|_{L^2(\partial\Omega)}^2 < \infty,$$

where $(-\Delta_S)^{s/2}$ is the fractional order spherical Laplace operator on the unit sphere. Since spherical harmonics, say $\{Y_n^m\}_{n \in \mathbb{N}_0, |m| \leq n}$, constitute an orthonormal basis of $L^2(\partial\Omega)$ (see for example [14]), we may expand $f \in L^2(\partial\Omega)$ as

$$f = \sum_{n=0}^{\infty} \sum_{m=-n}^n \langle f, Y_n^m \rangle Y_n^m, \quad \langle f, Y_n^m \rangle = \int_{\partial\Omega} f(x) \overline{Y_n^m(x)} d\sigma(x).$$

The spherical harmonics are eigenvectors of $(-\Delta_S)$, in particular,

$$(-\Delta_S)^{s/2} Y = (n(n+1))^{s/2} Y,$$

for any spherical harmonic Y of degree n . Then the requirement (32) gives rise to a characterization of $H^s(\partial\Omega)$ suitable for $s \in \mathbb{R}$ as those functions $f \in L^2(\partial\Omega)$ that satisfy

$$\sum_{n=0}^{\infty} \sum_{m=-n}^n (1+n^2)^s |\langle f, Y_n^m \rangle|^2 < \infty.$$

See [39, Chapter 1.7] for a more general treatment and the case $s < 0$. Thus we define the $H^s(\partial\Omega)$ inner products as

$$\langle f, g \rangle_s := \langle f, g \rangle_{H^s(\partial\Omega)} = \sum_{n=0}^{\infty} \sum_{m=-n}^n w_s(n) \langle f, Y_n^m \rangle \overline{w_s(n) \langle g, Y_n^m \rangle},$$

where the multiplier functions are defined as

$$w_s(n) := (1+n^2)^{s/2}, \quad \text{for } n \in \mathbb{N}_0, s \in \mathbb{R},$$

and hence $\|f\|_{H^s(\partial\Omega)} = \langle f, f \rangle_s^{1/2}$. We build an orthonormal basis $\{\phi_{n,m}^s\}_{n \in \mathbb{N}_0, |m| \leq n}$ of $H^s(\partial\Omega)$ with

$$\phi_{n,m}^s = w_{-s}(n) Y_n^m.$$

and hence any $g \in H^s(\partial\Omega)$ has the expansion

$$g = \sum_{n=0}^{\infty} \sum_{m=-n}^n \langle g, \phi_{n,m}^s \rangle_s \phi_{n,m}^s.$$

Consider the $L^2(\partial\Omega)$ orthogonal projection P_N to the space spanned by spherical harmonics of degree less than or equal to N , as

$$P_N g = \sum_{n=0}^N \sum_{m=-n}^n \langle g, Y_n^m \rangle Y_n^m.$$

Note $\langle g, Y_n^m \rangle$ as an integral over the unit sphere may be approximated by coefficients $c_{n,m}(\underline{g})$ using Gauss-Legendre quadrature in $2(N+1)^2$ appropriately chosen quadrature points $\{x_k\}_{k=1}^{2(N+1)^2}$ on the unit sphere as in [17]. Here we denote $\underline{g} = (g(x_1), \dots, g(x_{2(N+1)^2}))$. Define

$$L_N g := \sum_{n=0}^N \sum_{m=-n}^n c_{n,m}(\underline{g}) Y_n^m.$$

We may approximate any operator $\Lambda : H^s(\partial\Omega) \rightarrow H^{-s}(\partial\Omega)$ using Q , a matrix in $\mathbb{C}^{2(N+1)^2 \times 2(N+1)^2}$ defined by

$$(33) \quad (\Lambda g)(x_k) \simeq [Q\underline{g}]_k := \sum_{n=0}^N \sum_{m=-n}^n c_{n,m}(\underline{g}) (\Lambda Y_n^m)(x_k), \quad k = 1, \dots, 2(N+1)^2.$$

From here it is clear we can write Q as

$$(34) \quad Q = \tilde{Q}A,$$

where $A : g \mapsto (c_{0,0}(g), \dots, c_{N,N}(g))$, and $[\tilde{Q}]_{k\ell} = \Lambda Y_\ell(x_k)$, where Y_ℓ is the ℓ 'th spherical harmonic in the natural order. We can think of A as the matrix that takes a point-cloud representation of a function on $\partial\Omega$ and gives the spherical harmonic representation.

Similarly to [35], an approximation of the operator norm then takes the form

$$(35) \quad \|\Lambda\|_{s,-s} \simeq \sup_f \frac{\|\mathcal{Q}f\|_{\mathbb{C}^{(N+1)^2}}}{\|f\|_{\mathbb{C}^{(N+1)^2}}} = \|\mathcal{Q}\|_N,$$

where $[\mathcal{Q}]_{ij} = \langle \Lambda \phi_{n,m}^s, \phi_{n',m'}^{-s} \rangle_{-s}$ with $i = n'^2 + n' + m' + 1$ and $j = n^2 + n + m + 1$. We may approximate

$$(36) \quad \begin{aligned} \langle \Lambda \phi_{n,m}^s, \phi_{n',m'}^{-s} \rangle_{-s} &= w_{-s}(n) w_{-s}(n') \langle \Lambda Y_n^m, Y_{n'}^{m'} \rangle, \\ &\simeq w_{-s}(n) w_{-s}(n') c_{n',m'}(\Lambda Y_n^m). \end{aligned}$$

With \mathcal{B} we denote the map that takes the matrix Q and gives the approximation of \mathcal{Q} defined by (36). For $\Lambda = \Lambda_\gamma$ we denote the approximation (33), Q_γ .

From (33) it is clear that to represent Λ_γ we need only to compute $(\Lambda_\gamma Y_n^m)(x_k)$ in the quadrature points x_k . In this paper we compute $(\Lambda_\gamma Y_n^m)(x_k)$ efficiently by the boundary integral approach for piecewise constant conductivities given in [17], an approach which despite the lack of reconstruction theory has shown to perform well.

5.2. Noise model. We simulate a perturbation of the Dirichlet-to-Neumann map by adding Gaussian noise to Q_γ . We let

$$(37) \quad Q_\gamma^\varepsilon = Q_\gamma + \delta E,$$

where $\delta > 0$ and the elements of the $2(N+1)^2 \times 2(N+1)^2$ matrix E are independent Gaussian random variables with zero mean and unit variance. We modify E such that $\mathcal{B}E$ has a first row and column as zeros, such that we may consider $\mathcal{B}E$ as an approximation of a linear and bounded operator $\mathcal{E} \in Y$. Furthermore, we approximate $\|\mathcal{E}\|_Y$ using (35) and (36) and note we can specify an absolute level of noise $\|\mathcal{E}\|_Y \approx \varepsilon$ by choosing δ appropriately. The relative noise level is then

$$\delta \frac{\|\mathcal{E}\|_Y}{\|\Lambda_\gamma\|_Y} \approx \delta \frac{\|\mathcal{B}E\|_N}{\|\mathcal{B}Q_\gamma\|_N}.$$

Note the noise model in [17] scales each element of E with the corresponding element of Q_γ . Noise models for electrode data simulation typically takes the form

$$V_j^\varepsilon = V_j + \delta_j E_j,$$

as in [26], where V_j is the voltage vector corresponding to the j 'th current pattern, $\delta_j > 0$ is a scaling parameter dependent on V_j and E_j is a Gaussian vector independent of $E_{j'}$ for $j \neq j'$. For our case such a noise model corresponds best to adding to \tilde{Q}_γ in (34) a matrix \tilde{E} whose columns are $\delta_j E_j$. One may check by vectorizing $A^T \tilde{E}^T$ that the corresponding E of (37) consists of independent and identically distributed Gaussian vectors as rows. However, the elements of each row are now correlated with covariance matrix $A^T \text{diag}(\delta) A$.

Finally, we define the signal-to-noise ratio as

$$\text{SNR} = \frac{1}{(N+1)^2} \sum_{n=0}^N \sum_{m=-n}^n \frac{\|Q_\gamma Y_n^m\|_{\mathbb{C}^{2(N+1)^2}}}{\delta \|E Y_n^m\|_{\mathbb{C}^{2(N+1)^2}}}.$$

5.3. Solving the boundary integral equations. Following [17] we discretize the perturbed boundary integral equations (15) by

$$(38) \quad [I + (\mathcal{S}_0 L_N + \mathcal{H}_\zeta^N)(\Lambda_\gamma^\varepsilon - \Lambda_1) L_N] ((\psi_\zeta^N)^\varepsilon|_{\partial\Omega}) = e_\zeta|_{\partial\Omega},$$

where \mathcal{H}_ζ^N is the approximation of the integral operator $\mathcal{S}_\zeta - \mathcal{S}_0$ using the Gauss-Legendre quadrature rule of order $N+1$ on the unit sphere in the aforementioned quadrature points $\{x_k\}_{k=1}^{2(N+1)^2}$. We find the following result regarding the convergence of the perturbed solutions $(\psi_\zeta^N)^\varepsilon$ of (38) analogously to [16, 17].

Theorem 5.1. *Suppose $D < |\zeta(\xi)| < -\frac{1}{6} \log \varepsilon_2$ and \mathcal{E} is a linear bounded operator from $H^s(\partial\Omega)$ to $H^t(\partial\Omega)$ for all $s \geq 1/2$ and $t > s$. Then for all $s > 3/2$, there exists $N_0 \in \mathbb{N}$ such that for all $N \geq N_0$ the operator $I + (\mathcal{S}_0 L_N + \mathcal{H}_\zeta^N)(\Lambda_\gamma^\varepsilon - \Lambda_1) L_N$ is invertible in $H^s(\partial\Omega)$. Furthermore we have,*

$$\|(\psi_\zeta^N)^\varepsilon - \psi_\zeta^\varepsilon\|_{H^s(\partial\Omega)} \leq \frac{C}{N^{s-3/2}} \|e_\zeta\|_{H^s(\partial\Omega)}.$$

Proof. The result follows from a Neumann series argument as in Lemma 3.1 and Theorem 3.2 of [17] as for $D < |\zeta(\xi)| < -\frac{1}{6} \log \varepsilon_2$, there exists a bounded inverse $(B_\zeta^\varepsilon)^{-1}$ by Lemma 3.3. \square

This result ensures that the solutions of the discretized perturbed boundary integral equations are unique and converge to the solutions of (15).

5.4. Choice of $|\zeta(\xi)|$ and truncation radius. It is clear from Method 3 that we should set $|\zeta(\xi)| = M^p$ for some exponent $p > 3/2$. Due to the high sensitivity of the CGO solutions with respect to $|\zeta(\xi)|$, we may choose $|\zeta(\xi)|$ differently in practice, although we will not necessarily have a regularization strategy in theory. One idea of [16] is to set $|\zeta(\xi)|$ minimal in the admissible set (13), that is

$$|\zeta(\xi)| = \frac{M}{\sqrt{2}}.$$

A different idea is to choose $|\zeta(\xi)|$ independently for each ξ such that $|\zeta(\xi)|$ is minimal with $|\zeta(\xi)| = \frac{|\xi|}{\sqrt{2}}$. We take the critical choice $|\zeta(\xi)| = K_1 M^{3/2}$ for some constant $0 < K_1 < 1$ to maintain the smallest $|\zeta|$ within the boundaries of the theory.

In practice we compute $\mathbf{t}_{M(\varepsilon)}(\xi, \zeta(\xi))$ in a ξ -grid of points $|\xi| \leq M$ as in [17]. The Shannon sampling theorem ensures we can recover uniquely the inverse Fourier transform if we sample densely enough. We use the discrete Fourier transform in equidistant ξ - and x -grids in three dimensions.

$$\xi_k^j = -M + k \frac{2M}{K-1} \quad \text{and} \quad x_n^j = -x_{\max} + n \frac{2x_{\max}}{K-1},$$

for $n, k = 0, \dots, K-1$, $j = 1, 2, 3$ and some x_{\max} determined by K and M . Indeed the discrete Fourier transform requires

$$M = \frac{\pi(K-1)^2}{2Kx_{\max}}.$$

to recover $q^\varepsilon(x_n^j)$ for all $n = 0, \dots, K-1$, $j = 1, 2, 3$. In practical applications, we do not know the noise level, in which case we choose M and K and consequently determine x_{\max} . Then we recover q^ε in an appropriate finite element mesh of the unit ball using trilinear interpolation. The discrete Fourier transform is computed efficiently with the use of FFT [23] with complexity $\mathcal{O}(K^3 \log K^3)$.

The problem of finding the optimal truncation radius given noisy data $\Lambda_\gamma^\varepsilon$ is largely open and is related to the problem of systematically choosing a regularization parameter of regularized reconstruction for an inverse problem. In this paper, we choose the truncation radius by inspection for the simulated data. For further details on the implementation of the reconstruction algorithm we refer to [16, 17].

6. Numerical results. We test Method 2 as a regularization strategy. We are interested in whether the reconstruction converges to the true conductivity distribution as the noise level goes to zero, and likewise as the regularization parameter α goes to zero for a non-noisy Dirichlet-to-Neumann map. To this end, we simulate a Dirichlet-to-Neumann map for a well-known phantom.

6.1. Test phantom. The piecewise constant heart-lungs phantom consists of two spheroidal inclusions and a ball inclusion embedded in the unit sphere with a background conductivity of 1. The phantom is summarized in Table 1. We compute and represent the Dirichlet-to-Neumann map and noisy counterparts as described in Section 5.1. In particular, the forward map is computed using $2(N+1)^2$ boundary points on the unit sphere and using maximal degree N of spherical harmonics with $N = 25$.

Inclusion	Center	Radii	Axes	Conductivity
Ball	$(-0.09, -0.55, 0)$	$r = 0.273$		2
Left spheroid	$0.55(-\sin(\frac{5\pi}{12}), \cos(\frac{5\pi}{12}), 0)$	$r_1 = 0.468,$ $r_2 = 0.234,$ $r_3 = 0.234$	$(\cos(\frac{5\pi}{12}), \sin(\frac{5\pi}{12}), 0),$ $(-\sin(\frac{5\pi}{12}), \cos(\frac{5\pi}{12}), 0),$ $(0, 0, 1)$	0.5
Right spheroid	$0.45(\sin(\frac{5\pi}{12}), \cos(\frac{5\pi}{12}), 0)$	$r_1 = 0.546,$ $r_2 = 0.273,$ $r_3 = 0.273$	$(\cos(\frac{5\pi}{12}), -\sin(\frac{5\pi}{12}), 0),$ $(\sin(\frac{5\pi}{12}), \cos(\frac{5\pi}{12}), 0),$ $(0, 0, 1)$	0.5

TABLE 1. Summary of piecewise constant heart-lungs phantom consisting of three inclusions

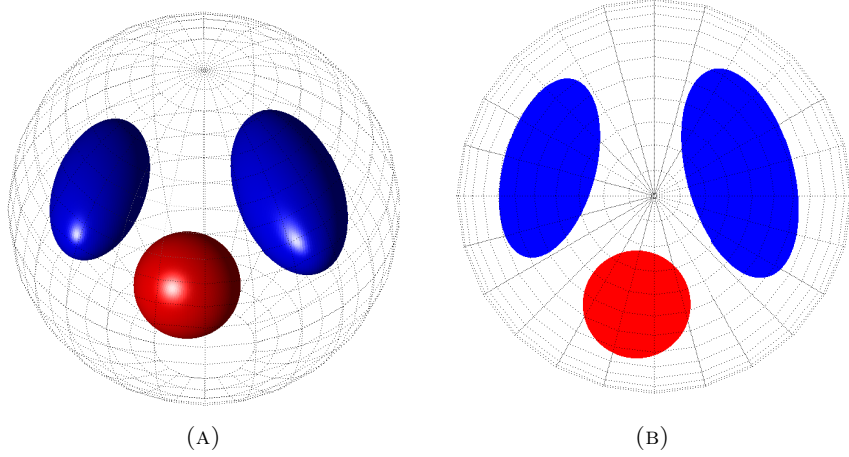


FIGURE 1. The piecewise constant heart-lungs phantom in a three-dimensional view (A), and in the planar cross section $x^3 = 0$ (B).

6.2. Regularization in practice. We now consider the regularization strategy, Method 2, in practice. Alluding to (2), we test the reconstruction algorithm by keeping the test data fixed and varying the regularization parameter. In Figure 2, we see cross-sectional plots of reconstructed conductivities for different truncation radii $M = \alpha^{-1}$. We use $|\zeta(\xi)| = \frac{1}{4}M^{3/2}$ as the critical choice such that $\zeta(\xi) \in \mathcal{V}_\xi$ for $M \geq 8$, and use the accurate Dirichlet-to-Neumann map with no added noise. The figure shows increasing accuracy and contrast for increasing truncation radii. Similar to the findings of [17], we experience failing reconstructions for large enough truncation radii as the frequency data is dominated by exponentially amplified noise inherent to the finite-precision representation of Λ_γ . This happens since there is noise present in the representation of the Dirichlet-to-Neumann map, no matter how accurately it represents the true infinite-precision data. We see the effect of truncation in practice: low resolution, smaller dynamical range and more smoothness caused by the missing high frequency data. Though not immediately clear from this figure, the reconstructions slightly overshoot the conductivity of the resistive spheroidal inclusions with conductivities as small as 0.38. In addition, the reconstruction algorithm seems to work well in practice on piecewise constant conductivity distributions.

In Figure 3, we see cross-sectional plots of reconstructed conductivities using Dirichlet-to-Neumann maps with added noise and for fixed $|\zeta(\xi)| = \frac{1}{3\sqrt{2}}M^{3/2}$. Here, K_1 is chosen such that $\zeta(\xi)$ is small and admissible for $M \geq 9$. The truncation radii are chosen optimally by visual inspection. The figure shows reconstructions in the presence of noise of levels ranging from $\varepsilon = 10^{-6}$ to $\varepsilon = 10^{-3}$ in the Dirichlet-to-Neumann map. We see improving quality of reconstruction as the noise level decreases in accordance with Definition 1. Beyond noise levels of 10^{-3} , reconstruction is still feasible without the corruption of unstable noise, although, they need heavy regularization and start to lack visible features of the phantom. In Figure 4, we see the conductivity reconstruction using noisy data with $\varepsilon = 10^{-2}$ corresponding to approximately 1% relative noise. The resistive spheroidal inclusions start to connect and the conductive spherical inclusion is not as accurately placed. The

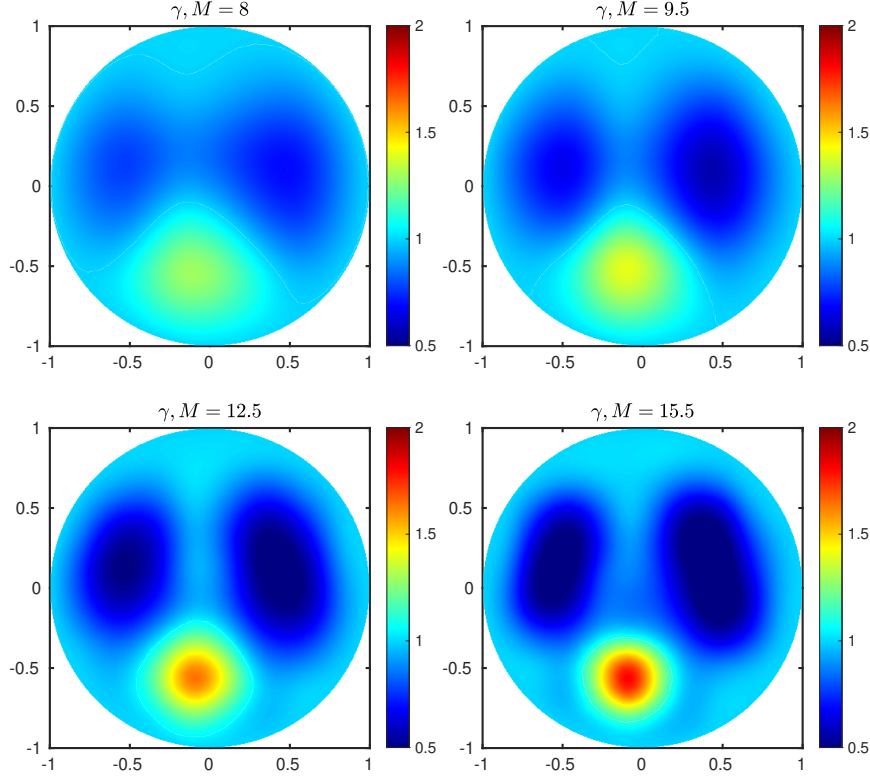


FIGURE 2. Cross sections ($x^3 = 0$) of reconstructions using the regularized reconstruction algorithm with different choices of truncation radius M , $K = 12$ and $|\zeta(\xi)| = \frac{1}{4}M^{3/2}$. There is no added noise.

remaining intensity in the signal compared to the case $M = 9.7$ in Figure 4 could suggest that additional regularization is needed.

The truncation radii of reconstructions in Figure 3 and 4 chosen by visual inspection are plotted and compared to the theoretically predicted truncation radius in Figure 5. This comparison suggests the prediction is somewhat pessimistic and that the practical algorithm allows for lighter regularization in comparison to what the theoretical estimates portend. However, the prediction and practical reconstructions are not directly comparable, since we should pick $|\zeta(\xi)| = K_1 M^p$ with p strictly larger than $3/2$ according to theory. Finally, we note the noise model utilized by [17] and [26] give somewhat different results compared to our unnormalized perturbation. The results also raise the question of how practical the reconstruction method is for more realistic data. Had we decreased the resolution of the basis of spherical harmonics to which voltages and currents are projected, the approximation error of highly oscillatory functions would increase. In this case we can expect to pick the truncation radius smaller to get a stable reconstruction. Investigating the reconstruction method for electrode data is subject to further study and is related to [29] for the two-dimensional D-bar method and [26] for the three-dimensional so-called \mathbf{t}^{exp} approximation. Possible improvements to the truncation strategy

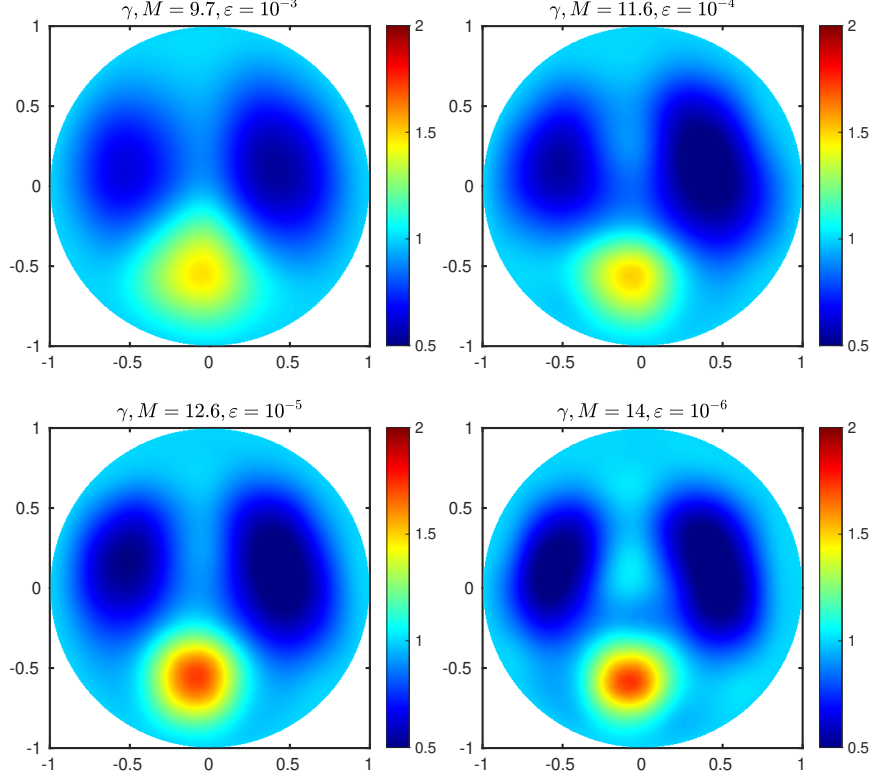


FIGURE 3. Cross sections ($x^3 = 0$) of reconstructions using the regularized reconstruction algorithm on noisy Dirichlet-to-Neumann maps. The noise levels correspond to relative noise levels $\varepsilon \approx 0.1\%$ with $\text{SNR} = 12 \cdot 10^3$ (top left), $\varepsilon \approx 0.01\%$ with $\text{SNR} = 123 \cdot 10^3$ (top right), $\varepsilon \approx 0.001\%$ with $\text{SNR} = 1172 \cdot 10^3$ (bottom left) and $\varepsilon \approx 0.0001\%$ with $\text{SNR} = 11299 \cdot 10^3$ (bottom right). The parameters used are $K = 11$ and $|\zeta(\xi)| = \frac{1}{3\sqrt{2}}M^{3/2}$.

include extending the support of \mathbf{t} with prior information using the forward map as in [5]. In addition, one could experiment with a truncation by thresholding as in [27].

7. Conclusions. In this paper we provide and investigate a regularization strategy for the Calderón problem in three dimensions. The main result of the paper is Theorem 1.1, which shows that the algorithm defined by Method 3 yields reconstructions approximating the true conductivity, when using data corrupted by a sufficiently small perturbation. The proof relies on a gap of the magnitude of the complex frequency in which the existence of unique CGO solutions is guaranteed and the noise level allows a stable and unique solution to the boundary integral equation. The reconstructions from this strategy are regular as a result of the spectral filtering. Numerical results show the regularizing behavior of the reconstruction algorithm in practice and suggests one can utilize higher frequency information in

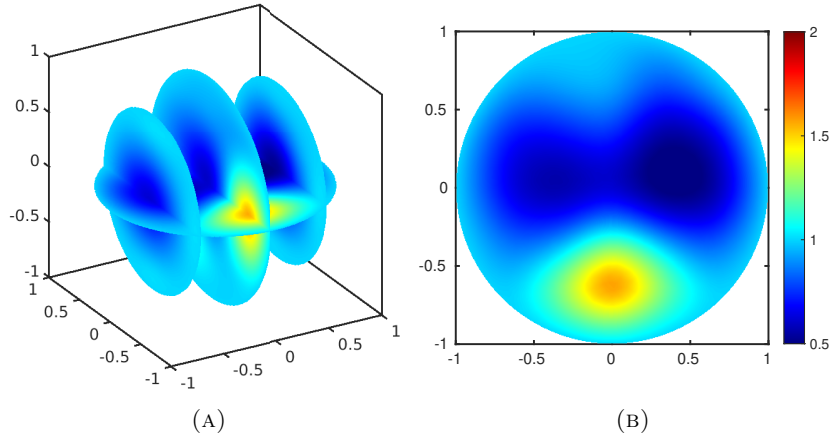


FIGURE 4. Regularized reconstruction using noisy Dirichlet-to-Neumann maps with $\varepsilon = 10^{-2}$, which corresponds to approximately 1% relative noise and $\text{SNR} = 1.17 \cdot 10^3$. Plot (A) shows the cross sections $x^3 = 0$, $x^2 = -0.6$, $x^2 = -0.05$ and $x^2 = 0.6$, whereas plot (B) shows the plane corresponding to $x^3 = 0$. The parameters used are $M = 9$, $K = 11$ and $|\zeta(\xi)| = \frac{1}{3\sqrt{2}} M^{3/2}$.

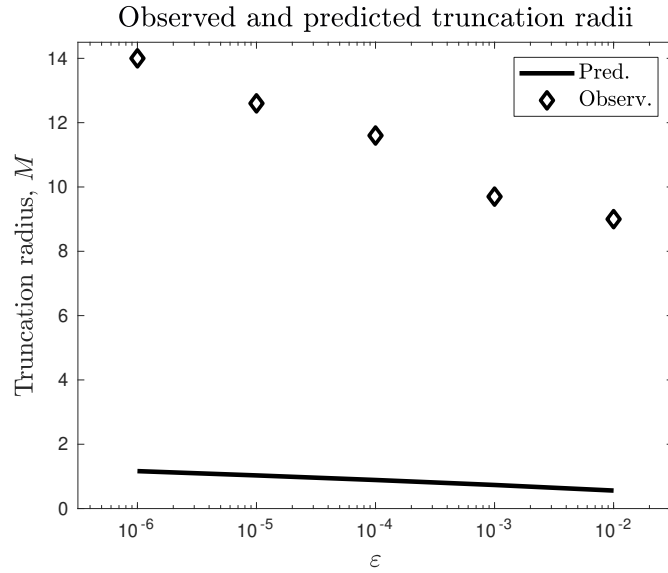


FIGURE 5. The truncation radii as predicted by theory $M = (-1/11 \log(\varepsilon))^{-1/p}$ for $p = 3/2$, and the chosen truncation radii for the noisy reconstructions of Figure 3 and 4.

the data than suggested by the theory. The reconstructions of piecewise constant conductivity data show promise even in the case of 1% relative noise.

Acknowledgments. AKR and KK were supported by The Villum Foundation (grant no. 25893).

REFERENCES

- [1] K. Abraham and R. Nickl, On statistical Calderón problems, *Math. Stat. Learn.*, **2** (2019), 165–216.
- [2] A. Adler, R. Amyot, R. Guardo, J. Bates and Y. Berthiaume, [Monitoring changes in lung air and liquid volumes with electrical impedance tomography](#), *Journal of Applied Physiology*, **83** (1997), 1762–1767.
- [3] G. Alessandrini, [Stable determination of conductivity by boundary measurements](#), *Appl. Anal.*, **27** (1988), 153–172.
- [4] G. Alessandrini, [Singular solutions of elliptic equations and the determination of conductivity by boundary measurements](#), *J. Differential Equations*, **84** (1990), 252–272.
- [5] M. Alsaker and J. L. Mueller, [A D-bar algorithm with a priori information for 2-dimensional electrical impedance tomography](#), *SIAM J. Imaging Sci.*, **9** (2016), 1619–1654.
- [6] K. Astala and L. Päivärinta, [Calderón’s inverse conductivity problem in the plane](#), *Ann. of Math. (2)*, **163** (2006), 265–299.
- [7] J. Bikowski, K. Knudsen and J. L. Mueller, [Direct numerical reconstruction of conductivities in three dimensions using scattering transforms](#), *Inverse Problems*, **27** (2011), 015002, 19 pp.
- [8] G. Boverman, T.-J. Kao, D. Isaacson and G. J. Saulnier, [An implementation of Calderón’s method for 3-D Limited-View EIT](#), *IEEE Transactions on Medical Imaging*, **28** (2009), 1073–82.
- [9] R. M. Brown, [Global uniqueness in the impedance-imaging problem for less regular conductivities](#), *SIAM J. Math. Anal.*, **27** (1996), 1049–1056.
- [10] A.-P. Calderón, On an inverse boundary value problem, in *Seminar on Numerical Analysis and its Applications to Continuum Physics (Rio de Janeiro, 1980)*, Soc. Brasil. Mat., Rio de Janeiro, 1980, 65–73.
- [11] P. Caro and A. Garcia, [The Calderón problem with corrupted data](#), *Inverse Problems*, **33** (2017), 085001, 17 pp.
- [12] P. Caro and K. M. Rogers, [Global uniqueness for the Calderón problem with Lipschitz conductivities](#), *Forum. Math. Pi*, **4** (2016), e2, 28 pp.
- [13] V. Cherepenin, A. Karpov, A. Korjenevsky, V. Kornienko, Y. Kultiasov, M. Ochapkin, O. Trochanova and J. Meister, [Three-dimensional EIT imaging of breast tissues: System design and clinical testing](#), *IEEE Transactions on Medical Imaging*, **21** (2002), 662–667.
- [14] D. Colton and R. Kress, *[Inverse Acoustic and Electromagnetic Scattering Theory](#)*, vol. 93 of Applied Mathematical Sciences, Springer-Verlag, Berlin, 1992.
- [15] H. Cornean, K. Knudsen and S. Siltanen, [Towards a \$d\$ -bar reconstruction method for three-dimensional EIT](#), *J. Inverse Ill-Posed Probl.*, **14** (2006), 111–134.
- [16] F. Delbary, P. C. Hansen and K. Knudsen, [Electrical impedance tomography: 3D reconstructions using scattering transforms](#), *Appl. Anal.*, **91** (2012), 737–755.
- [17] F. Delbary and K. Knudsen, [Numerical nonlinear complex geometrical optics algorithm for the 3D Calderón problem](#), *Inverse Probl. Imaging*, **8** (2014), 991–1012.
- [18] D. C. Dobson, [Convergence of a reconstruction method for the inverse conductivity problem](#), *SIAM J. Appl. Math.*, **52** (1992), 442–458.
- [19] M. Dunlop and A. Stuart, [The Bayesian formulation of EIT: Analysis and algorithms](#), *Inverse Probl. Imaging*, **10** (2016), 1007–1036.
- [20] H. W. Engl, M. Hanke and A. Neubauer, *[Regularization of Inverse Problems](#)*, vol. 375 of Mathematics and its Applications, Kluwer Academic Publishers Group, Dordrecht, 1996.
- [21] L. C. Evans, *[Partial Differential Equations](#)*, vol. 19, American Mathematical Society, 2010.
- [22] I. Frerichs and T. Becher, [Chest electrical impedance tomography measures in neonatology and paediatrics - a survey on clinical usefulness](#), *Physiological Measurement*, **40** (2019), 054001.
- [23] M. Frigo and S. G. Johnson, [The design and implementation of FFTW3](#), *Proceedings of the IEEE*, **93** (2005), 216–231.
- [24] N. Goren, J. Avery, T. Dowrick, E. Mackle, A. Witkowska-Wrobel, D. Werring and D. Holder, [Multi-frequency electrical impedance tomography and neuroimaging data in stroke patients](#), *Scientific Data*, **5** (2018), 180112, 10 pp.

- [25] M. Hallaji, A. Seppänen and M. Pour-Ghaz, [Electrical impedance tomography-based sensing skin for quantitative imaging of damage in concrete](#), *Smart Materials and Structures*, **23** (2014), 085001.
- [26] S. J. Hamilton, D. Isaacson, V. Kolehmainen, P. A. Muller, J. Toivainen and P. F. Bray, [3D electrical impedance tomography reconstructions from simulated electrode data using direct inversion \$t^{\text{exp}}\$ and Calderón methods](#), *Inverse Probl. Imaging*, **15** (2021), 1135–1169.
- [27] A. Hauptmann, M. Santacesaria and S. Siltanen, [Direct inversion from partial-boundary data in electrical impedance tomography](#), *Inverse Problems*, **33** (2017), 025009, 26 pp.
- [28] T. C. Hou and J. P. Lynch, [Electrical impedance tomographic methods for sensing strain fields and crack damage in cementitious structures](#), *Journal of Intelligent Material Systems and Structures*, **20** (2009), 1363–1379.
- [29] D. Isaacson, J. Mueller, J. Newell and S. Siltanen, [Reconstructions of chest phantoms by the d-bar method for electrical impedance tomography](#), *IEEE Transactions on Medical Imaging*, **23** (2004), 821–828.
- [30] B. Jin and P. Maass, [An analysis of electrical impedance tomography with applications to Tikhonov regularization](#), *ESAIM Control Optim. Calc. Var.*, **18** (2012), 1027–1048.
- [31] J. P. Kaipio, V. Kolehmainen, E. Somersalo and M. Vauhkonen, [Statistical inversion and Monte Carlo sampling methods in electrical impedance tomography](#), *Inverse Problems*, **16** (2000), 1487–1522.
- [32] A. Kirsch, [An Introduction to the Mathematical Theory of Inverse Problems](#), vol. 120 of Applied Mathematical Sciences, 2nd edition, Springer, New York, 2011.
- [33] K. Knudsen, [A new direct method for reconstructing isotropic conductivities in the plane](#), *Physiological Measurement*, **24** (2003), 391–401.
- [34] K. Knudsen, M. Lassas, J. L. Mueller and S. Siltanen, [D-bar method for electrical impedance tomography with discontinuous conductivities](#), *SIAM J. Appl. Math.*, **67** (2007), 893–913.
- [35] K. Knudsen, M. Lassas, J. L. Mueller and S. Siltanen, [Regularized D-bar method for the inverse conductivity problem](#), *Inverse Probl. Imaging*, **3** (2009), 599–624.
- [36] K. Knudsen and J. L. Mueller, The Born approximation and Calderón’s method for reconstruction of conductivities in 3-D, *Discrete Contin. Dyn. Syst.*, 8th AIMS Conference. Suppl. Vol. II, 2011, 844–853.
- [37] A. Lechleiter and A. Rieder, [Newton regularizations for impedance tomography: Convergence by local injectivity](#), *Inverse Problems*, **24** (2008), 065009, 18 pp.
- [38] S. Leonhardt and B. Lachmann, [Electrical impedance tomography: The holy grail of ventilation and perfusion monitoring?](#), *Intensive Care Medicine*, **38** (2012), 1917–1929.
- [39] J.-L. Lions and E. Magenes, *Non-Homogeneous Boundary Value Problems and Applications. Vol. I*, Springer-Verlag, New York-Heidelberg, 1972, Translated from the French by P. Kenneth, Die Grundlehren der mathematischen Wissenschaften, Band 181.
- [40] E. Malone, M. Jehl, S. Arridge, T. Betcke and D. Holder, [Stroke type differentiation using spectrally constrained multifrequency EIT: Evaluation of feasibility in a realistic head model](#), *Physiological Measurement*, **35** (2014), 1051–1066.
- [41] N. Mandache, [Exponential instability in an inverse problem for the Schrödinger equation](#), *Inverse Problems*, **17** (2001), 1435–1444.
- [42] J. L. Mueller and S. Siltanen, [Direct reconstructions of conductivities from boundary measurements](#), *SIAM J. Sci. Comput.*, **24** (2003), 1232–1266.
- [43] J. L. Mueller, S. Siltanen and D. Isaacson, [A direct reconstruction algorithm for electrical impedance tomography](#), *IEEE Transactions on Medical Imaging*, **21** (2002), 555–559.
- [44] A. I. Nachman, [Reconstructions from boundary measurements](#), *Ann. of Math. (2)*, **128** (1988), 531–576.
- [45] A. I. Nachman, [Global uniqueness for a two-dimensional inverse boundary value problem](#), *Ann. of Math. (2)*, **143** (1996), 71–96.
- [46] A. Nachman, J. Sylvester and G. Uhlmann, [An \$n\$ -dimensional Borg-Levinson theorem](#), *Comm. Math. Phys.*, **115** (1988), 595–605.
- [47] R. G. Novikov, [Multidimensional inverse spectral problem for the equation \$-\Delta\psi + \(v\(x\) - Eu\(x\)\)\psi = 0\$](#) , *Functional Analysis and its Applications*, **22** (1988), 263–272.
- [48] M. Reed and B. Simon, *Methods of Modern Mathematical Physics 1, Functional Analysis*, Academic Press, 1980.
- [49] L. Rondi, [On the regularization of the inverse conductivity problem with discontinuous conductivities](#), *Inverse Probl. Imaging*, **2** (2008), 397–409.

- [50] L. Rondi, [Discrete approximation and regularisation for the inverse conductivity problem](#), *Rend. Istit. Mat. Univ. Trieste*, **48** (2016), 315–352.
- [51] M. Salo, [Semiclassical pseudodifferential calculus and the reconstruction of a magnetic field](#), *Comm. Partial Differential Equations*, **31** (2006), 1639–1666.
- [52] C. Schmidt, S. Wagner, M. Burger, U. V. Rienen and C. H. Wolters, [Impact of uncertain head tissue conductivity in the optimization of transcranial direct current stimulation for an auditory target](#), *Journal of Neural Engineering*, **12** (2015), 046028.
- [53] S. Siltanen, J. Mueller and D. Isaacson, [Erratum: “An implementation of the reconstruction algorithm of A. Nachman for the 2D inverse conductivity problem \[Inverse Problems 16 \(2000\), 681–699\]”](#), *Inverse Problems*, **17** (2001), 1561–1563.
- [54] S. Siltanen, J. Mueller and D. Isaacson, [An implementation of the reconstruction algorithm of A. Nachman for the 2D inverse conductivity problem](#), *Inverse Problems*, **16** (2000), 681–699.
- [55] P. Soltan, *A Primer on Hilbert Space Operators*, Springer International Publishing, 2018.
- [56] J. Sylvester and G. Uhlmann, [A global uniqueness theorem for an inverse boundary value problem](#), *Ann. of Math. (2)*, **125** (1987), 153–169.
- [57] Y. Zhao, E. Zimmermann, J. A. Huisman, A. Treichel, B. Wolters, S. Van Waasen and A. Kemna, [Broadband EIT borehole measurements with high phase accuracy using numerical corrections of electromagnetic coupling effects](#), *Measurement Science and Technology*, **24** (2013), 085005.
- [58] Y. Zou and Z. Guo, [A review of electrical impedance techniques for breast cancer detection](#), *Medical Engineering and Physics*, **25** (2003), 79–90.

E-mail address: kiknu@dtu.dk

E-mail address: akara@dtu.dk